Investigation of Characteristics of Separation Zones in T-Junctions

HAMID SHAMLOO *, BAHAREH PIRZADEH**
Civil Engineering Department
K.N Toosi University of Technology
No.1346 Valiasr Street, Tehran
IRAN
*hshamloo@yahoo.com, ** b.pirzadeh@gmail.com

Abstract: The river diversion, for domestic, agricultural and industrial consumption, has a vital role to make economic progress and to develop the human communities. There are different ways of river diversion which are proportional to rivers' condition and the quantity of the diversion of water. Lateral river intake is one of these ways. This paper provides detail application of FLUENT-2D software in simulation of lateral intake flows. Numerical simulations undertaken in present two dimensional work use RSM turbulent model. Results of velocity field measurement using K-ε Standard model were compared with Shettar & Murthy (1966). Then using RSM turbulent model, dimensions of separation zone were measured and compared with Kasthuri & Pundarikanthan (1987). In both cases good agreement are found between numerical and experimental results.

Key-Words: Open channel, Lateral Intake, Turbulence, Separation zone, Numerical modeling, Fluent

1 Introduction

In hydraulic and environmental engineering, one commonly comes across branching channel flows. Some of distinctive characteristics of a dividing flow in an open channel are illustrated in Fig.1. A zone of separation near the entrance of the branch channel, a contracted flow region in the branch channel, and a stagnation point near the downstream corner of the junction can be observed. In the region downstream of the junction, along the continuous far wall, separation due to flow expansion may occur (Ramamurthy et al. 2007).

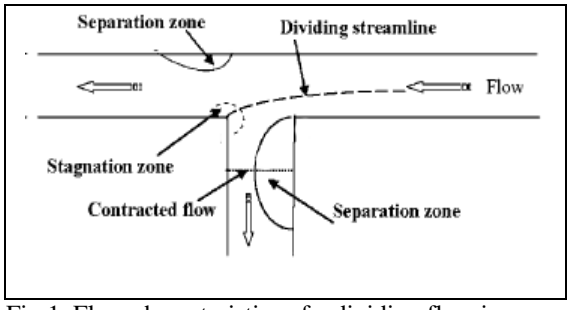

Fig.1. Flow characteristics of a dividing flow in open channels

Flows through lateral intakes adjoining rivers and canals are turbulent. The transverse pressure gradients in the vicinity of the intake induce region of mean-velocity gradients, depth-varying surface of flow division and separation, vortices, and zone of flow reversal.

As the flow approaches the intake, it accelerates laterally by the suction pressure at the end of branch channel. This may cause the flow to divide into two portions, one entering the branched channel and the other flowing downstream in the main channel. The diverted flow experiences an imbalance between the transverse pressure gradient and shear and centrifugal forces indicating a clockwise secondary motion cell (Neary et al. 1999).

A great number of experimental and analytical studies are dealt with dividing flows. Taylor (1944) conducted the first detailed experimental study in an open channel and proposed a graphical solution, which included a trial-and-error procedure. Grace and Priest (1958) presented experimental results for division of the flow with different width ratios of the branch channel to the main channel. They also classified division of the flow into two regimes, with and without the appearance of local standing waves near the branch. The regime without waves corresponded to the case where the Froude numbers were relatively small, and the regime with waves corresponded to the free over-fall conditions at

sections downstream of the junction. Without the appearance of standing waves, the downstream-to-upstream depth ratio and the branch-to-downstream depth ratio were nearly equal to unity and ratios mildly decreased while the branch-to-main channel upstream discharge ratio increased.

Law and Reynolds (1966) investigated the problem of dividing flows using analytical and experimental methods. They concluded that for a dividing flow at low Froude numbers in a right-angled dividing flow, the momentum and energy principles can both be applied to describe the flow in the main channel extension.

Existing results (Krishnappa and Seetharamiah 1963; Law 1965; Sridharan 1966; Ramamurthy and Satish 1988) indicate that the flow condition at the entrance to the branch is generally unsubmerged when the Froude number F_r in the branch is greater than a threshold value (0.3 or 0.35). This feature becomes important in correlating discharge distribution with other flow parameters. When the flow at the section of maximum contraction is un-submerged, division of the flow at the junction is relatively unaffected by changes in the downstream section of the branch channel.

For branching channels or intakes, result obtained from different researchers (Kasthuri and Pundarikhathan 1987; Best and Reid (1984); Neary et al 1999) indicate that both length and width of the separation zone decrease with increasing the discharge ratio.

Shettar and Murthy (1996) deployed depth-averaged mean flow equations associated by the standard k-ε model. Results obtained from their model for an open channel T-junction showed that for discharge ratio 0.52, a good agreement between measurements and model results can be obtained.

Ramamurthy et al. (2007) presented experimental data related to 3D mean velocity components and water surface profiles for dividing flows in open channels. The data set presented in their paper was composed of water surface mappings and 3D velocity distributions in the vicinity of the channel junction region.

Dimensions of separation zone obtained from the current 2D-numerical model were compared with those of Kasthuri and Pundarikanthan's experiments (1987). Velocity field measurements were compared with measured velocities of Shettar and Murthy (1996).

2 Importance of Study

Appropriate sediment control at water intakes is one of the primary goals of their design. The storage volume of any sedimentation chamber downstream has to last as long as possible and, in the case of a hydro power plant, the turbines must be protected from the incoming sediments. The design of an intake has traditionally been refined by carrying out physical model studies. It has recently become more popular to improve the design process using the result from a numerical model study. Applying computational fluid dynamics (CFD) in this field of engineering can improve the final design and accelerate the design process. Also it is importance lies in the fact that the analysis of the junctions is of considerable use to engineers engaged on the design of irrigation systems, storm sewers, channel in sewerage treatment works, power installations and other similar projects.

The topic of the present study is the use of 2-D numerical model to predict the velocity profile and dimension of separation zone in the flow approaching a water intake.

3 Experimental Results

Dimension of separation zone obtained from the current numerical model were compared with laboratory experiment results performed by Kasthuri and Pundarikanthan (1987) and Velocity profiles obtained from the current numerical model were compared with laboratory experiment results performed by Shettar and Murthy (1996).

In both experimental set-up, the main channel was 6m long and the intake was 3m long, fitted at its midpoint. The width of both channels (b) was 0.3m, the bed slope was zero and channels were 0.25m deep, as illustrated in Fig.2. The channel bed was finished with smooth cement plaster and walls were built from Perspex sheets.

In Kasthuri and Pundarikanthan's experimentsl (1987) flows were subcritical during all runs and the Froude number in inlet varying from 0.1 to 0.4. They have presented relationships between the maximum non-dimensional length (S_L/b) and non-dimensional width (S_W/b) of the separation zone, and $R=Q_b/Q$ (Q is the total discharge in the upstream boundary of the main channel, Q_b is the intake discharge).

In Shettar and Murthy's experiments (1996) the discharge ration was 0.52 and the Froude number at inlet was 0.54 so the velocity at inlet was 0.85m/s.

They presented depth-averaged mean velocity profiles in different sections across the main and intake channel.

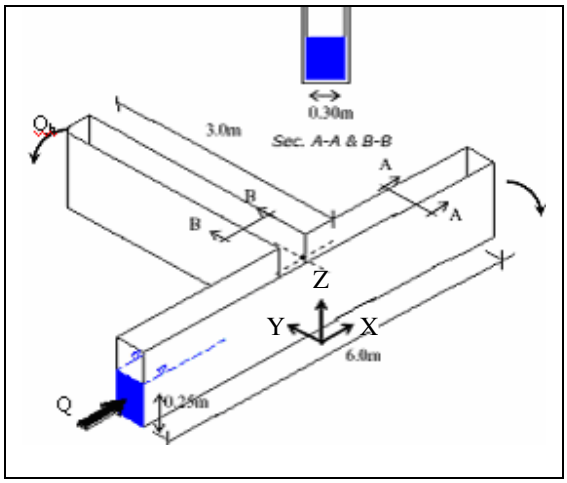

Fig2. Layout of main channel and intake

4 Numerical Model Description

FLUENT is the CFD solver of choice for complex flow ranging from incompressible (transonic) to highly compressible (supersonic and hypersonic) flows. It Provide multiple solver options, combined with a convergence-enhancing multi-grid method, FLUENT delivers optimum solution efficiency and accuracy for a wide range of speed regimes (Fluent user guide 2003).

FLUENT solves governing equations sequentially using the control volume method. The governing equations are integrated over each control volume to construct discrete algebraic equations for dependent variables. These discrete equations are linearized using an implicit method.

Turbulent flows can be simulated in FLUENT using the standard K-ε, LES, RNG, or the Reynolds-stress (RSM) closure schemes. The model optimizes computational efficiency by allowing the user to choose between various spatial (Second-order upwind, first-order, QUICK) discritization scheme.

We used second order upwind discritization scheme for Pressure, Momentum, Turbulent kinetic energy and turbulent dissipation rate and used SIMPLE algorithm for Pressure-Velocity Coupling Method.

For these problems, the conversions creations in Fluent (Scaled Residuals) decreases to 10^{-6} for all equations (Fig.3).

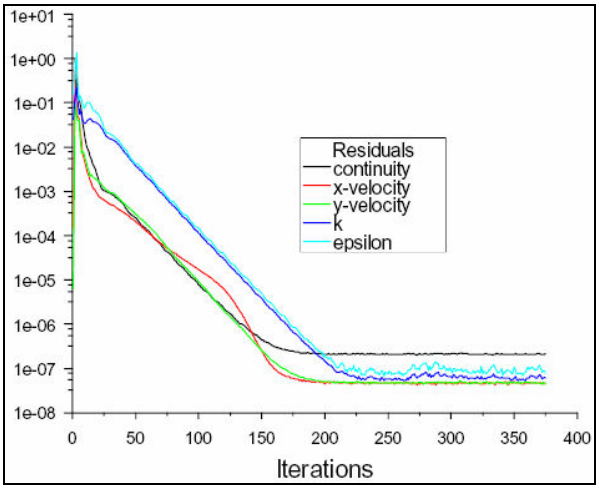

Fig3. Scaled Residuals

5 Governing equations

The governing equations of fluid flow in rivers and channels are generally based on three-dimensional Reynoldes averaged equations for incompressible free surface unsteady turbulent flows as follows [2]:

$$\frac{\partial U_i}{\partial t}+U_j\frac{\partial U_i}{\partial x_j}=\frac{1}{\rho}\frac{\partial}{\partial x_j}\left[\left(-P+\frac{2}{3}k\right)\delta_{ij}+\nu_T\left(\frac{\partial U_i}{\partial x_J}+\frac{\partial U_j}{\partial x_i}\right)\right] \quad (1)$$

There are basically five terms: a transient term and a convective term on the left side of the equation. On the right side of the equation there is a pressure/kinetic term, a diffusive term and a stress term.

In the current study, it is assumed that the density of water is constant through the computational domain. The governing differential equations of mass and momentum balance for unsteady free surface flow can be expressed as [8,9]:

$$\frac{\partial u_i}{\partial x_i}=0 \quad (2)$$

$$\frac{\partial u_i}{\partial t}+u_j\frac{\partial u_i}{\partial x_j}=-\frac{1}{\rho}\frac{\partial P}{\partial x_i}+g_{xi}+\upsilon\nabla^2 u_i \quad (3)$$

Where t=time; u_i is the velocity in the x_i direction; P is the pressure; ν is the molecular viscosity; g_{xi} is the gravitational acceleration in the x_i direction, and ρ is the density of flow.

As in the current study, only the steady state condition has been considered, therefore equation (2) to (3) incorporate appropriate initial and

boundary conditions deployed to achieve equilibrium conditions.
Under-relaxation factors are chosen between 0.2 and 0.5. The small value of under-relaxation factors is required for the stability of the solution of interpolation scheme.

The simplest and most widely used two-equation turbulence model is the k-ε model that solves two separate equations to allow the turbulent kinetic energy and dissipation rate to be independently determined.

The turbulence kinetic energy, *k*, is modeled as:

$$\frac{\partial k}{\partial t}+U_j\frac{\partial k}{\partial x_j}=\frac{\partial}{\partial x_j}\left(\frac{\nu_T}{\sigma_k}\frac{\partial k}{\partial x_j}\right)+P_k-\varepsilon \tag{4}$$

Where P_k is given by:

$$P_k=\nu_T\frac{\partial U_j}{\partial x_i}\left(\frac{\partial U_j}{\partial x_i}+\frac{\partial U_i}{\partial x_j}\right) \tag{5}$$

$$\nu_T=c_\mu\frac{k}{\varepsilon^2} \tag{6}$$

The dissipation of k is denoted ε, and modeled as:

$$\frac{\partial \varepsilon}{\partial t}+U_j\frac{\partial \varepsilon}{\partial x_j}=\frac{\partial}{\partial x_j}\left(\frac{\nu_T}{\sigma_k}\frac{\partial \varepsilon}{\partial x_j}\right)+C_{\varepsilon 1}\frac{\varepsilon}{k}P_k+C_{\varepsilon 2}\frac{\varepsilon^2}{k} \tag{7}$$

The constants in the k-ε model have the following values: $c\mu=0.09$, $c_{\varepsilon 1}=1.44$, $c_{\varepsilon 2}=1.92$, $\sigma_k=1.0$ and $\sigma_\varepsilon=1.30$
The Reynolds stress model (RSM) provides closure of the Reynolds-averaged Navier-Stokes equations by solving transport equations for Reynoldes stresses and an equation for energy dissipation rate (four-equation for 2D flows and seven-equation for 3D flows). Since the RSM accounts for the effects of streamline curvature, swirl, rotation, and rapid changes in strain rate in a more rigorous manner than one-equation and two-equation models, it has greater potential to give accurate predictions for complex flows.
The exact transport equations for the transport of the Reynolds stresses, $\rho\overline{u_i'u_j'}$, may be written as follows:

$$\frac{\partial}{\partial t}(\rho\overline{u_i'u_j'})+\frac{\partial}{\partial x_k}\left(\rho u_k\overline{u_i'u_j'}\right)=-\frac{\partial}{\partial x_k}\left[\rho\overline{u_i'u_j'u_k'}+p\left(\delta_{kj}u_i'+\delta_{ik}u_j'\right)\right]+$$
$$\frac{\partial}{\partial x_k}\left[\mu\frac{\partial}{\partial x_k}\left(\overline{u_i'u_j'}\right)\right]-\rho\left(\overline{u_i'u_k'}\frac{\partial u_j}{\partial x_k}+\overline{u_j'u_k'}\frac{\partial u_i}{\partial x_k}\right)-\rho\beta\left(g_i\overline{u_j'\theta}+g_j\overline{u_i'\theta}\right)$$
$$+\overline{p\left(\frac{\partial u_i'}{\partial x_j}+\frac{\partial u_j'}{\partial x_i}\right)}-2\mu\overline{\frac{\partial u_i'}{\partial x_k}\frac{\partial u_j'}{\partial x_k}}-2\rho\Omega_k\left(\overline{u_j'u_m'}\varepsilon_{ikm}+\overline{u_i'u_m'}\varepsilon_{jkm}\right)+s_{user} \tag{8}$$

6 Boundary conditions

Appropriate conditions must be specified at domain boundaries depending on the nature of the flow.
Outflow boundary condition used for two outlets at all of runs. The length of the main and branch channels were chosen properly; therefore sufficient distance is provided between the junction and two outlets to ensure that the flow returned to the undisturbed pattern. The no-slip boundary condition is specified to set the velocity to be zero at the solid boundaries and assumed to be smooth.
In simulation performed in the first case of present study, velocity inlet boundary condition is specified, and set to 0.85 m/s for comparing velocity across the main channel and branch corresponding to the Shettar & Murthy experiments. In this case Discharge ratios $R=Q_b/Q$ equal to 0.52 (as used by Shettar and Murthy-1996) was used.
In the second case, velocity inlet boundary condition set to 0.5m/s to provide similar Experimental Froude number with Kasthuri and Pundarikanthan experiments. In this case Seven discharge ratios $R=Q_b/Q$ equal to 0.2, 0.35, 0.45, 0.52, 0.65, 0.80 and 0.90 were used.
It is also important to establish that grid-independent results have been obtained. The grid structure must be fine enough especially near the wall boundaries and the junction, which is the region of rapid variation. Various flow computational trials have been carried out with different number of grids in x and y directions. It was found that results are independent of grid size, if at least 3550 nodes are used (Pirzadeh 2007). Computational mesh is shown in Fig.4.

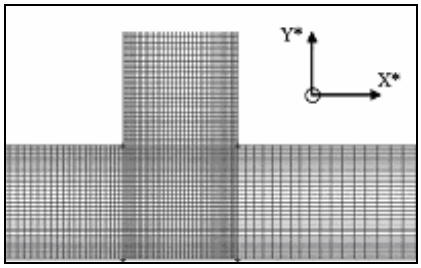

Fig.4. Computational geometry and grid

7 Results and Discussions

7-1- velocity field

In the first case of this paper numerical investigations are performed for evolution of the ability of an available 2D flow solver to cop with the fully turbulent flow in a T-junction.

In the Fig.(5) to (14) results of the numerical model are compared with experimental depth averaged velocity profiles in the main and the branch channel at 10 no dimensional locations at x and y direction.

From these figures, it can be concluded that results generally have reasonable agreement with measured ones, but at some sections (especially in branch channel) computed results do not agree very well with those measured, which might be partly due to the three dimensional effects. Further, Shettar and Murthy (1996) presented depth-averaged mean flow velocities but in the current 2D-study surface velocities have been used.

As the flow approaches the branch inlet, the building up of transverse slop implies a negative pressure gradient accompanied by fluid acceleration near the inner wall and positive pressure gradient accompanied by fluid deceleration near the outer wall (Fig.15). The forward velocity maximum shift towards the inner banks as the flow inters the inlet region. As the flow starts entering into the branch, the resultant velocity along the inlet reduces and hence, at the downstream edge of the inlet, forward velocity maximum shift away from the inner wall. The flow remaining in the main channel expand to the full width of the main channel and due to the curvature already attained by it at the junction region, flow is directed towards the inner wall and again the velocity maximum shift towards it(Fig.16).

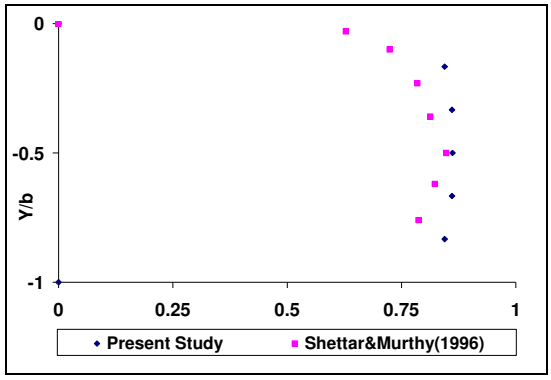

Fig5. X-Velocity Profile in the Main channel (X*=-5.50)

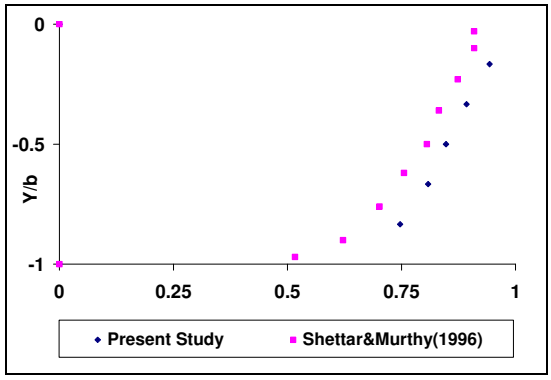

Fig6. X-Velocity Profile in the Main channel (X*=-0.50)

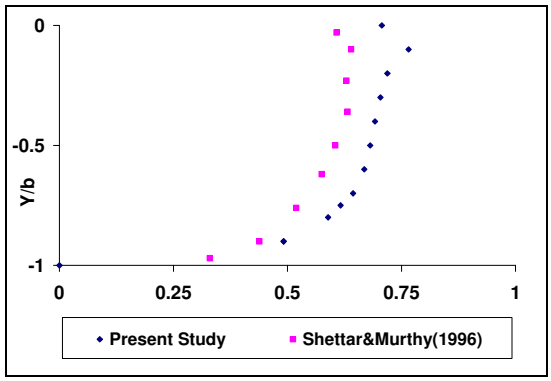

Fig7. X-Velocity Profile in the Main channel (X*=0.0)

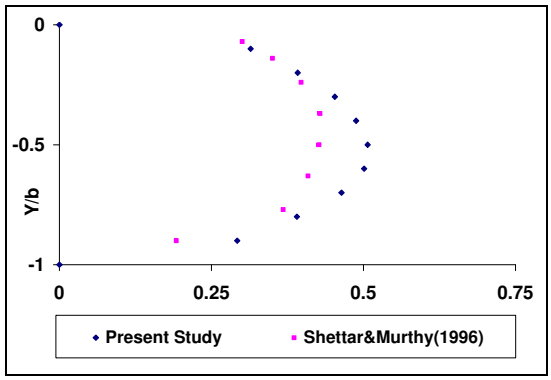

Fig8. X-Velocity Profile in the Main channel (X*=0.50)

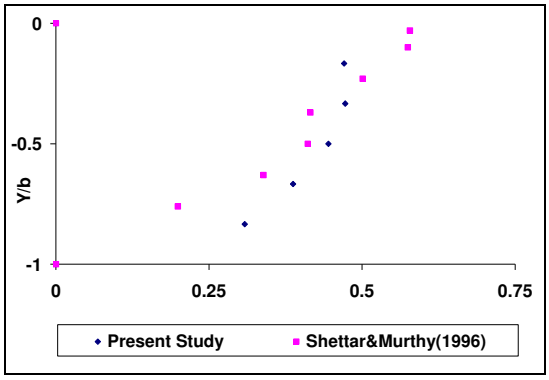

Fig9. X-Velocity Profile in the Main channel (X*=1.50)

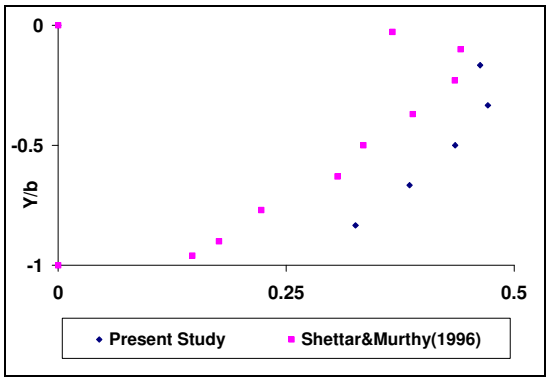

Fig10. X-Velocity Profile in the Main channel (X*=7.0)

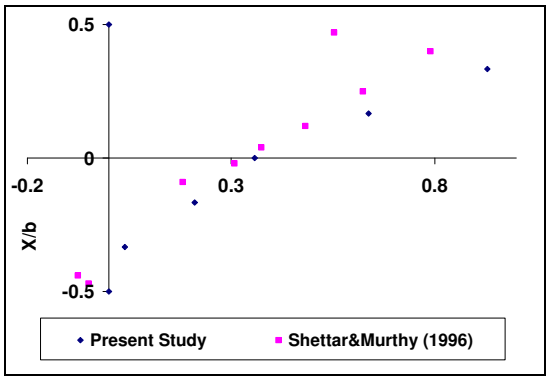

Fig11. Y-Velocity Profile in the Branch channel (Y*=0.65)

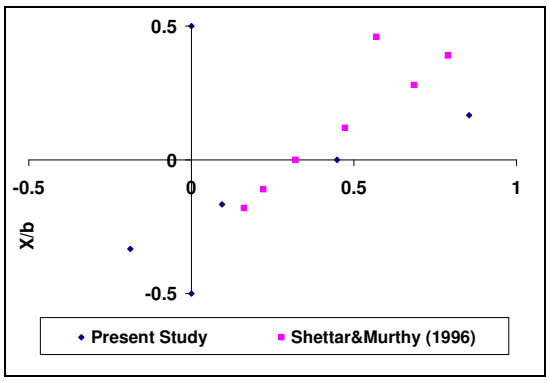

Fig12. Y-Velocity Profile in the Branch channel (Y*=1.65)

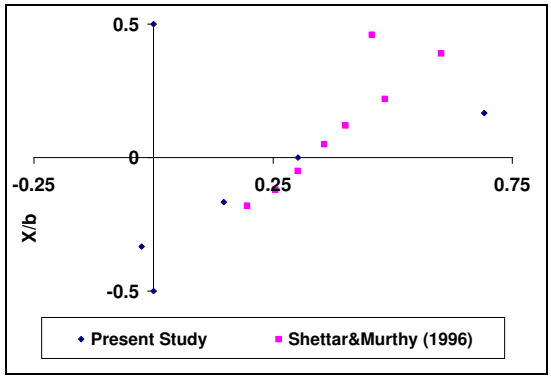

Fig13. Y-Velocity Profile in the Branch channel (Y*=2.65)

Fig14. Y-Velocity Profile in the Branch channel (Y*=3.65)

7-2- dimension of separation zone in the intake

In the second step at this study, numerical approaches were used to understand flow structure and separation zone at the water intake.

It was found that the size and location of separation zone is very much dependent on the discharge ratio. The result showed that for high discharge ratio the separation occurs in the downstream side of water intake whereas in low discharge ratio, it occurs in the upstream side.

Figs. (17) to (23) show 2D streamline plots. These plots elucidate the structure of the dividing stream surface and the zone of flow separation in intake. The flow at the junction can be divided into two regions; the region from which the branch channel abstracts the water and the region where the flow continues in the main channel. The streamline which divides these two regions is known as dividing streamline. However, the dividing streamline obtained in the present two-dimensional analysis should be viewed caution.

By comparing these figures, it is seen that an increase in discharge ratio causes shortening and narrowing of the separation zone.

A second separation zone may occur in the section of the main channel downstream of the junction because of flow expansion in this region. The width and length of the separation zone increase when R increases. When R is very small, the separation zone would not exist.

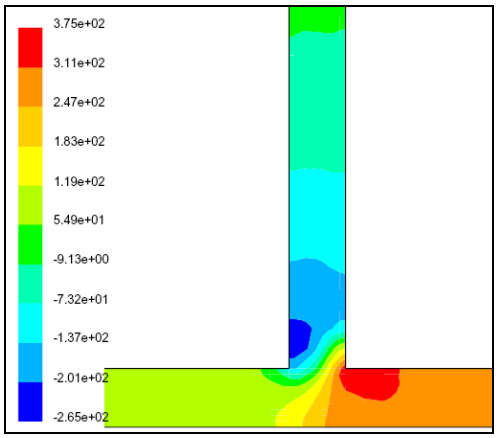

Fig15. Contours of predicted static pressure (Pascal)

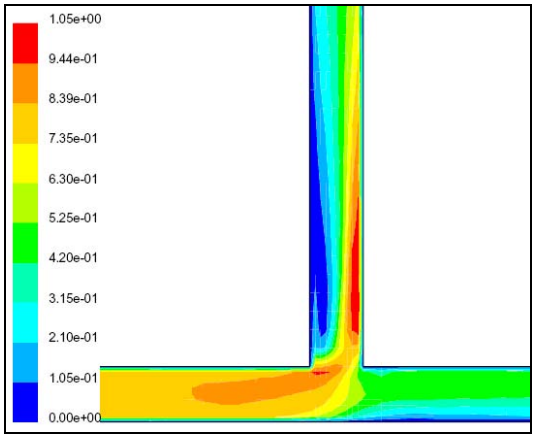

Fig16. Contours of predicted velocity magnitude (m/s)

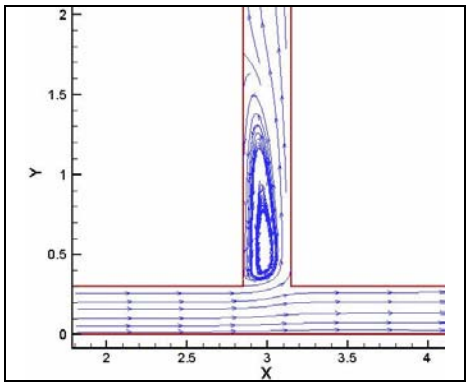

Fig.17. 2D Streamlines plot for R=0.20

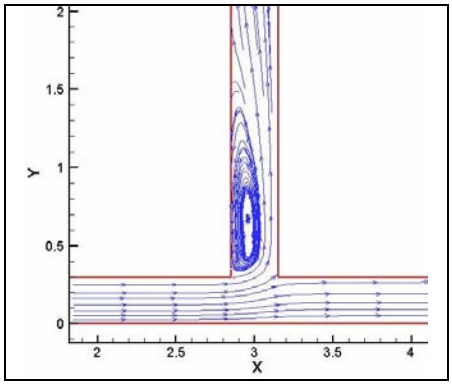

Fig.18. 2D Streamlines plot for R=0.35

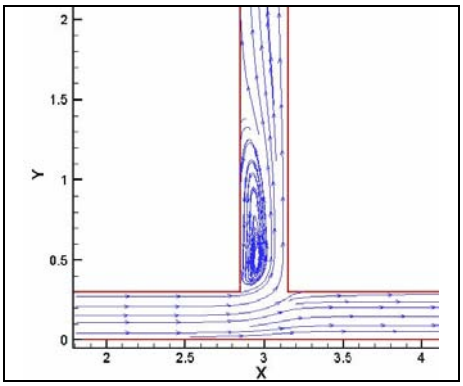

Fig.19. 2D Streamlines plot for R=0.45

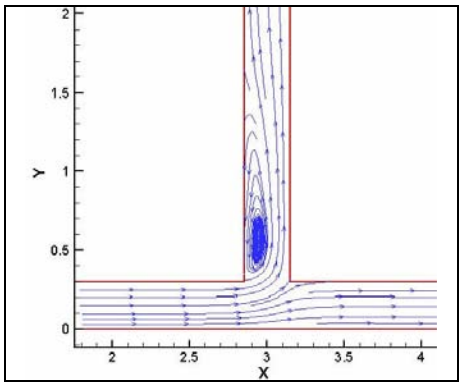

Fig.20. 2D Streamlines plot for R=0.52

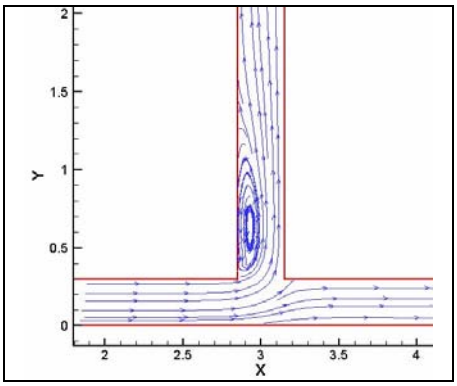

Fig.21. 2D Streamlines plot for R=0.65

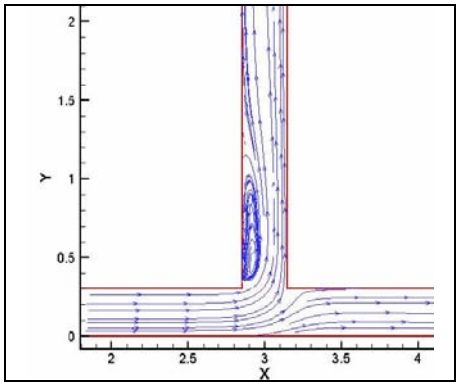

Fig.22. 2D Streamlines plot for R=0.80

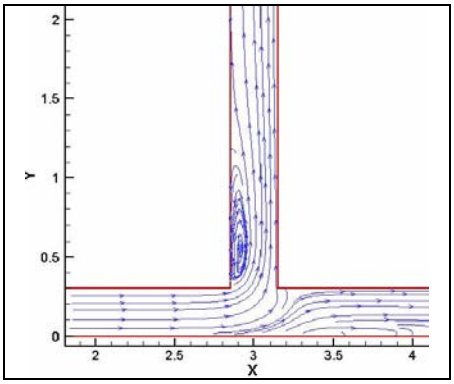

Fig.23. 2D Streamlines plot for R=0.90

Figs.(24) to (25) present the predicted variation of non-dimensional width and length of separation zone in the intake for different discharge ratios. Measurement of Kasthuri and Pundarikanthan (1987) is included for comparison. A good agreement is found between the experimental data and the present numerical results.

Results indicate that both length and width of the separation zone decrease with increasing discharge ratio. Separation zone reduces the effective width of the channel. Separation zone can be defined as the area of reduced pressure and re-circulating fluid with low velocities; therefore it has a strong sediment deposition potential in which sediment particles enter the branch channel. It can be seen that for a lower discharge ratio, more than 60% of the branch channel width is occupied by the re-circulating zone. Numerically, it is found that the recirculation region ends before the end of the branch channel.

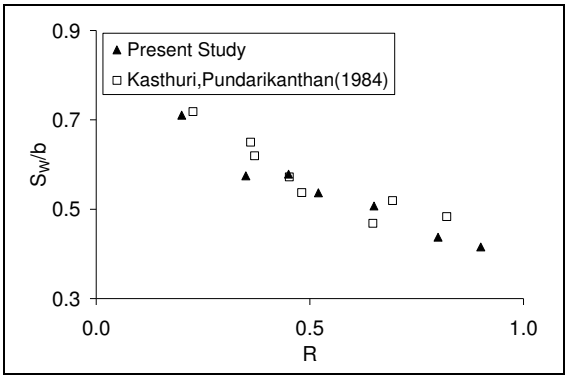

Fig.24. Dimensionless width separation zone vs. Ratio of discharge

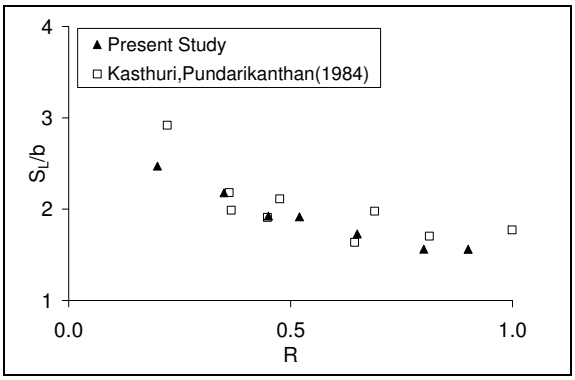

Fig.25. Dimensionless Length separation zone vs. Ratio of discharge

Fig.26. shows that the contraction coefficient Cc, (Cc=effective width of lateral intake/width of intake), increases linearly as discharge ratio increases. This indicates that a smaller branch discharge Q_b results in a small effective width in the recirculation region of the branch channel.

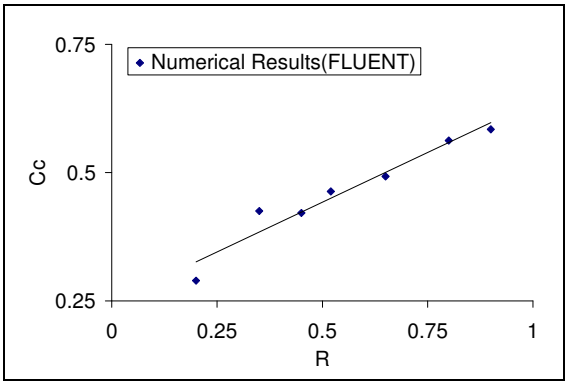

Fig26. Contraction coefficient in branch channel

8 Summary and Conclusions

Using lateral intake is a method of floodwater driving. In arid and semi-arid areas, floodwater contain large amount of sediment that will be carried into the intakes and decreases channel conveyance. Sediment conveys into the intake and settles in the separation zone beside the upstream side of lateral channel. Sedimentation in separation zone reduces the conveyance of lateral channel, thus it is important to determine the length and width of separation zone.

In this study the velocity components and dimensions of separation zone at the intake for dividing flows in a 90°, sharp-edged, rectangular open channel junction formed by channels of equal width are obtained on the basis of numerical studies. It was found the size and location of separation zone is very much dependent on the discharge ratio. In all cases, the results showed an increase in discharge ratio causes shorting and narrowing of the separation zone.

The largest Y-Velocities appear to occur just downstream of the branch near Y/b=1.0 for all discharge ratios simulated, where the maximum flow contraction occurs.

A separation zone may also occur in the main channel downstream of the junction, because of the flow expansion. The width and length of this separation zone increase with the increase in the discharge ratio zone increase with the increase in the discharge ratio R.

Notation

The following symbols are used in this paper:

b	=	width of both channel
t	=	time
$u_i = U_i$	=	represents velocity in the x_i direction
P	=	Total Pressure
$g_i = g_{xi}$	=	gravitational acceleration in the i (xi) direction
∂	=	Partial differential operator
ρ	=	average local density in the control volume computed
τ_{ij}	=	stress tensor
ν	=	Kinematics molecular viscosity
ν_t	=	Turbulent viscosity
K	=	Turbulently kinetic energy
δ_{ij}	=	Kronecker delta
Q_b	=	intake discharge
Q	=	total discharge in main channel upstream
R	=	Q_b/Q, discharge ratio
ε	=	dissipation rate
X	=	distance in main channel, downstream from branch channel centerline
Y	=	distance in branch channel from opposite main channel wall
X^*	=	X normalized by channel width
Y^*	=	Y normalized by channel width
S_W	=	Maximum width of separation zone in intake
S_L	=	Maximum width of separation zone in intake
C_c	=	Effective width of lateral intake / b

References

[1] BEST J.L., REID., "Separation zone at open channel junction.", *Journal of Hydraulic Engineering*, Vol.110, No.11, 1984,pp.1588-1594

[2] FLUENT user's guide manual-version 6.1., Fluent Incorporated, N.H., 2003

[3] GRACE J. L., and PRIEST, M. S," Division of flow in open channel junctions", Bulletin No. 31, Engineering Experimental Station, Alabama Polytechnic Institute, 1958.

[4] KASTHURI B. and PUNDARIKHANTHAN N.V, "Discussion on separation zone at open channel junction.", *Journal of Hydraulic Engineering*, Vol.113, No.4, 1987,pp.543-548

[5] KRISHNAPPA G., SEETHARAMIAH K.,"A new method of predicting the flow in a 90° branch channel.", La Houille Blanche, No.7, 1963

[6] LAW S.W., "Dividing flow in an open channel." Ms Thesis, McGill Univ., Montreal, Canada, 1965

[7] LAW, REYNOLDS, "Dividing flow in an open channel", *Journal of Hydraulic Div.* ,Vol.92, No2,1966, pp.4730-4736

[8] NEARY V.S., SOTIROPOULOUS F. and ODGAARD A.J., "Three-dimensional numerical model of lateral-intake inflows.", *Journal of Hydraulic Engineering*, Vol.125, No.2, 1999,pp.126-140

[9] NEARY V.S. and ODGAARD A.J., "Three-dimensional flow structure at open-channel diversions.", *Journal of Hydraulic Engineering*, Vol.119, No.11, 1993, pp. 1223-1230

[10] Pirzadeh B., "Numerical Investigation of Hydraulics of Lateral River Intakes", M.S.C thesis, K.N.Toosi University of technology, 2008

[11] RAMAMURTHY A.S, SATISH M.G, "Internal hydraulics of diffusers with uniform lateral momentum distribution. ", *Journal of Hydraulic Engineering*, Vol.113, No.3, 1987,pp.449-463

[12] RAMAMURTHY. A. S., JUNYING Qu; and DIEP VO., "Numerical and Experimental Study of Dividing Open-Channel Flows.", *Journal of Hydraulic Research*, Vol.133, No.10, 2007, pp.1135-1144

[13] SHETTAR A.S. and MURTHY K.K., "A Numerical study of division flow in open channels.", *Journal of Hydraulic Research*, Vol.34, No.5, 1996,pp.651-675

[14] Shamloo H., Pirzadeh B., "Investigation of Characteristics of Separation Zones in T-Junctions", Proceedings of the 12th WSEAS International Conference on APPLIED MATHEMATICS", Cairo, Egypt, Desember29-31, 2007, PP.189-193

[15] Shamloo H., Pirzadeh B., "Numerical investigation of Velocity Field in Dividing Open-Channel Flow", Proceedings of the 12th WSEAS International Conference on APPLIED *MATHEMATICS",* Cairo, Egypt, Desember29-31, 2007, PP.194-198

[16] SRIDHARAN K., "Division of flow in open channels.", Thesis, Indian Institute of Science, Bangalore, India, 1966

[17] TAYLOR, E.H. "Flow characteristics at rectangular open-channel junctions." *Trans. ASCE*, 109, 1944, pp. 893–902